

Excitation of surface plasmon-polaritons through optically-induced ultrafast transient gratings

Olesia Pashina,^{1,2} Olga Sergaeva,² Albert Seredin,² Giulia Crotti,³ Giuseppe Della Valle,³ Andrey Bogdanov,² Mihail Petrov,^{2,*} and Costantino De Angelis¹

¹*University of Brescia, Brescia, Italy*

²*School of Physics and Engineering, ITMO University, St. Petersburg 197101, Russia*

³*Polytechnic University of Milan, Milan, Italy*

Ultrafast excitation of non-equilibrium carriers under intense pulses offer unique opportunities for controlling optical properties of semiconductor materials. In this work, we propose a scheme for ultrafast generation of surface plasmon polaritons (SPPs) via a transient metagrating formed under two interfering optical pump pulses in the semiconductor GaAs thin film. The grating can be formed due to modulation of the refractive index associated with the non-equilibrium carriers generation. The formed temporal grating structure enables generation of SPP waves at GaAs/Ag interface via weak probe pulse excitation. We propose a theoretical model describing non-equilibrium carriers formation and diffusion and their contribution to permittivity modulation via Drude and band-filling mechanisms. We predict that by tuning the parameters of the pump and probe one can reach critical coupling regime and achieve efficient generation of SPP at the times scales of 0.1-1 ps.

I. INTRODUCTION

The recent progress in nonlinear all-dielectric nanophotonics [1–5] naturally stimulated active studies of all-optical modulation of semiconductor and dielectric nanostructures such as single scatterers [6, 7] and metasurfaces [8–16]. On this path, thermo-optical effect, probably, shows the largest values of Kerr-type nonlinearity leading to efficient modulation of linear and nonlinear light scattering [17–21] and reaching bistability regimes [22–25], but the modulation time scales can not be shorter than nanoseconds [22, 26]. At the same time, non-equilibrium carriers generation results in optical modulation at much shorter time scales ranging from hundreds of femtoseconds to picoseconds [27].

The ultrafast nonlinearity driven by the non-equilibrium carriers has been already utilized for Kerr-type self-induced modification of scattering of single semiconductor metaatoms [6, 7] and light reflection and transmission in metasurface structures [10, 11, 14, 16] including fast light modulation in anisotropic structures [15]. Besides the self-induced modulation of optical properties, all-optical ultrastrong modulation of all-dielectric metasurfaces was achieved in the pump-probe scheme [28–30] also with help of formation of polaritonic condensates in novel excitonic materials [31, 32].

The streamline strategy underlying the ultrafast all-optical manipulation and control of light is based on semiconductor nanostructures, such as single nanoantennas and metasurfaces, with pronounced resonant properties [1, 3, 33]: indeed, resonances allow to concentrate fields on subwavelength scales, granting superior modulation efficiency in compact structures with respect to non-resonant systems, e.g., thin films. On the other hand,

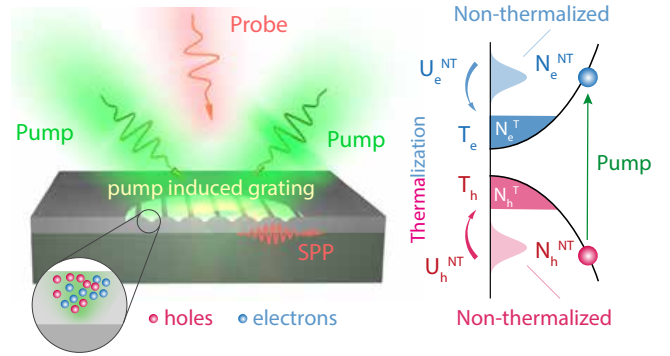


FIG. 1. Illustration of optically induced transient grating formation in GaAs film under the interference of pump fs-pulses with wavelength λ_{pump} . The grating is formed due to generation of non-equilibrium free-carriers under ultrashort pump excitation. Excitation of SPP wave at GaAs/Ag interface with probe pulse with wavelength λ_{pr} .

fabrication of nanometric components with optimal quality for applications still represents a challenge for manufacturer. Moreover, in terms of reconfigurability of the optical functionality, regardless the physical mechanism exploited for the reconfiguration (being electrical, thermal, or hot-carrier based), nanostructured materials pose a further substantial issue, i.e. the addressability of their individual nanoelements.

We present here a possible approach to tackle these limitations, based on the concept of spatial inhomogeneity in the photo-induced permittivity variation, which has been recently explored in metals [34–36]. We exploit non-uniform modulation of the permittivity in an initially homogeneous medium to obtain the formation of a transient nanophotonic structure. Specifically, we theoretically propose a strategy to induce an optical grating in a thin GaAs film by illuminating it with structured light. We then show how to exploit this phenomenon

* m.petrov@metalab.ifmo.ru

to excite surface plasmon-polaritons (SPPs) at the interface between the semiconductor thin film and a metallic medium.

The grating emergence is obtained with two crossed femtosecond pump pulses, whose interference grants a spatially periodic absorption pattern (see Fig. 1). In turn, this causes a periodic modulation of the permittivity $\Delta\varepsilon$ due to the non-equilibrium carriers' distribution: thus, the grating structure is transient, and exists at the time scale of carrier diffusion and recombination. In this ultrafast temporal window, SPPs can be excited at the GaAs/Ag interface with a probe pulse, as the diffraction grating allows to fulfil the necessary phase-matching condition [37].

To quantitatively discuss the key ideas presented above, we developed a theoretical description for the non-equilibrium carriers generation and transport dynamics at the nanoscale. Our self-consistent model represents a considerable expansion and improvement with respect to the approaches employed up-to-now to study the ultrafast response of semiconductor nanostructures, photo-excited with pulsed light.

II. THEORETICAL MODEL

Extended two-temperature model. Modeling of optically induced transient structures requires comprehensive analysis of free carrier generation, thermalization, diffusion, and recombination, as well as their interaction with the lattice phonons. The most common approach is based on the extended two-temperature (eTT) model [34], which has already been actively used for describing ultrafast dynamics in metals [34] and metallic nanostructures [38]. Here we utilize eTT to model the dynamics of nonequilibrium processes occurring within a GaAs film when subjected to ultrashort laser pulse irradiation. Specifically, generation of nonequilibrium electron and hole charge carriers are caused by optically induced interband transitions. While the detailed description of the theoretical model is provided in Supplemental Information, Section 1, here we will present the key aspects of the model.

The formed non-thermalized carriers are described by the concentration $N_e^{\text{NT}}(\mathbf{r}, t)$ and corresponding energy $\mathcal{U}_e^{\text{NT}}(\mathbf{r}, t)$ as shown in see Fig. 1. The Dember effect [39], which facilitates ambipolar diffusion of generated electrons and holes, enables us to assume that the evolution of charge carriers occurs in a nearly identical manner. Consequently, we can analyze our problem exclusively from the perspective of single charges, i.e. electrons. The subsequent carriers thermalization results in formation of their quasi-equilibrium distribution with temperature $T_e(\mathbf{r}, t)$ and concentration $N_e^{\text{T}}(\mathbf{r}, t)$. The further cooling of electron and hole subsystem due to interaction with phonons leads to increase of the lattice temperature $T_{ph}(\mathbf{r}, t)$. The model also accounts for non-thermalized and thermalized carrier diffusion and relaxation, as well

as for heat generation and diffusion. One can see the characteristic times of mentioned processes occurring in the structure in Table I.

The approach is based on the system of coupled differential equations describing the key characteristics dynamics with a spatiotemporal resolution (below each characteristic is assumed with (\mathbf{r}, t) dependence):

$$\begin{aligned} \frac{\partial \mathcal{U}_e^{\text{NT}}}{\partial t} &= \frac{1}{C_e} \nabla [k_e \nabla \mathcal{U}_e^{\text{NT}}] - (\Gamma_e + \Gamma_{ph}) \mathcal{U}_e^{\text{NT}} + Q_{\mathcal{U}_e}, \\ \frac{\partial N_e^{\text{NT}}}{\partial t} &= Q_{N_e} + \nabla [D \nabla N_e^{\text{NT}}] - \Gamma_e N_e^{\text{NT}}, \\ \frac{\partial N_e^{\text{T}}}{\partial t} &= \Gamma_e N_e^{\text{NT}} + \nabla [D \nabla N_e^{\text{T}}] - \\ &\quad (\gamma_{nr} N_e^{\text{T}} + \gamma_r N_e^{\text{T}2} + \gamma_{Au} N_e^{\text{T}3}), \\ \frac{\partial [C_e T_e]}{\partial t} &= \nabla [k_e \nabla T_e] - G_{e-ph} [T_e - T_{ph}] + \Gamma_e \mathcal{U}_e^{\text{NT}}, \\ \frac{\partial [C_{ph} T_{ph}]}{\partial t} &= \nabla [k_{ph} \nabla T_{ph}] + G_{e-ph} [T_e - T_{ph}] + \Gamma_{ph} \mathcal{U}_e^{\text{NT}}, \end{aligned} \quad (1)$$

Here Q_{N_e} and $Q_{\mathcal{U}_e}$ represent the concentration and energy sources characterized by optical absorption at each point of the structure defined by the imaginary part of the dielectric permittivity $\varepsilon(\mathbf{r}, t)$. The coefficients $C_{e/ph}$, $k_{e/ph}$, $\mu_{e/ph}$ correspond to the electron/phonon heat capacity, thermal conductivity, and mobility [40–42], respectively. Additionally, Γ_e denotes the rate of energy exchange between non-thermal and thermal electrons [43], while Γ_{ph} is the rate of energy transfer between electrons and phonons [44]. The electron-phonon relaxation time is given by G_{e-ph} [44, 45], and D is the coefficient for ambipolar heat diffusion [46]. Model also accounts for non-radiative decay γ_{nr} , radiative recombination γ_r and Auger recombination γ_{Au} in GaAs [47].

All coefficients in the system are dependent on the evolving parameters, which ultimately makes this approach complex and highly self-consistent. The self-consistency is also caused by the temporal modulation of dielectric permittivity and optical properties of structures, driven by the dynamics of carriers and phonons characteristics, which in terms changes the source functions Q_{N_e} and $Q_{\mathcal{U}_e}$.

Dielectric permittivity. We account altering of the dielectric constant of the material via two main effects: formation of free-electron gas accounted within the Drude model [49], and band-filling effect [50] related to the occupation of the states at the bottom of the conduction band (top of the valence band) with the free carriers (see more details in Supplemental Information Sec. 2). Thus, the dielectric constant of has two contributions associated with the Drude model and band-filling effect:

$$\begin{aligned} \varepsilon_{\text{fin}}(\mathbf{r}, t) &= [(n_0 + \Delta n_{bf}(\mathbf{r}, t)) + i(k_0 + \Delta k_{bf})(\mathbf{r}, t)]^2 + \dots \\ &\quad + \Delta \varepsilon_{Dr}(\mathbf{r}, t), \end{aligned} \quad (2)$$

where $n_0 + ik_0$ is the initial complex refractive index of

TABLE I. The characteristic time scales of various ultrafast processes underlying the two-temperature model of the GaAs material sorted in ascending order. These values are defined for electron temperatures $T_e = 300 - 10^4$ K and high-density electron-hole plasma $N_e = 10^{20} \text{ cm}^{-3}$ taking into account the characteristic nonuniformity length scale $d \approx 1 \mu\text{m}$. Here, electron-phonon scattering is related to $\Gamma^{T_e}(N_e) = G_{e-ph}(N_e)/C_e(N_e)$ and $\Gamma^{T_{ph}}(N_e, T_{ph}) = G_{e-ph}(N_e)/C_{ph}(T_{ph})$. The diffusion of electron concentration can be characterized by the concentration diffusion time $\tau_{\text{diff}}^{N_e} = \frac{d^2}{4\pi^2 D}$, while the heat diffusion coefficients for electrons and phonons are defined as $\tau_{\text{diff}}^{T_{e/ph}} = \frac{d^2}{4\pi^2 D_{e/ph}}$, where $D_{e/ph} = k_{e/ph}/C_{e/ph}$ [48] (See more details in Supplemental Information Sec. 1).

Effect	Characteristic time scale	Value
Thermalization of non-thermal electrons U_e^{NT}	$\tau_e = 1/\Gamma_e(T_e)$	≈ 200 fs
Evolution of electron temperature T_e due to electron-phonon scattering	$1/\Gamma^{T_e}(N_e)$	≈ 500 fs
Diffusion of electron temperature T_e	$\tau_{\text{diff}}^{T_e}(d, T_e)$	≈ 2 ps - 52 fs
Diffusion of electron concentration N_e	$\tau_{\text{diff}}^{N_e}(d, T_e)$	≈ 13 ps - 390 fs
Evolution of phonon temperature T_{ph} due to electron-phonon scattering	$1/\Gamma^{T_{ph}}(N_e)$	≈ 0.3 ns
Energy transfer between non-thermal electrons and phonons	$1/\Gamma_{ph}(N_e)$	≈ 0.3 ns
Diffusion of phonon temperature T_{ph}	$\tau_{\text{diff}}^{T_{ph}}(d)$	≈ 80 ns

GaAs [51], while the terms $\Delta n_{bf}(\mathbf{r}, t) + i\Delta k_{bf}(\mathbf{r}, t)$ and $\Delta \varepsilon_{Dr}(\mathbf{r}, t)$ represent the change of complex refractive index due to the band filling effect and the complex dielectric permittivity modulation based on Drude model, respectively. Within the model, we also assume that dielectric constant $\varepsilon(\mathbf{r}, t)$ varies in time slowly enough that we can consider the problem segregated manner and solving stationary Maxwell's equations at each time moment t . This approximation is valid for pulses of hundreds of femtosecond and optical systems with relatively low Q-factor, and self-consistent solution of Maxwell's equations along with a carrier dynamics equations may be required. However, our research indicates that accounting for this self-consistency in the context of ultrashort pulses (with femtosecond duration) is negligible, but for longer pulse duration the developed model is essential (See Supplemental Information Sec. 4B).

Finally, we implemented our theoretical model within the COMSOL Multiphysics simulation package (See Supplemental Information Sec. 3) by linking Maxwell equations with diffusion equations describing carriers dynamics in a self-consistent manner. This allows us to explore the connection between the electromagnetic field distribution $\mathbf{E}(\mathbf{r}, t)$ within the semiconduc-

tor material and the evolution of the key parameters ($U_e^{\text{NT}}(\mathbf{r}, t), N_e^{\text{NT}}(\mathbf{r}, t), N_e^{\text{T}}(\mathbf{r}, t), T_e(\mathbf{r}, t), T_{ph}(\mathbf{r}, t)$) resulting in the overall variation of the optical constants and change in optical properties of the photonic structure.

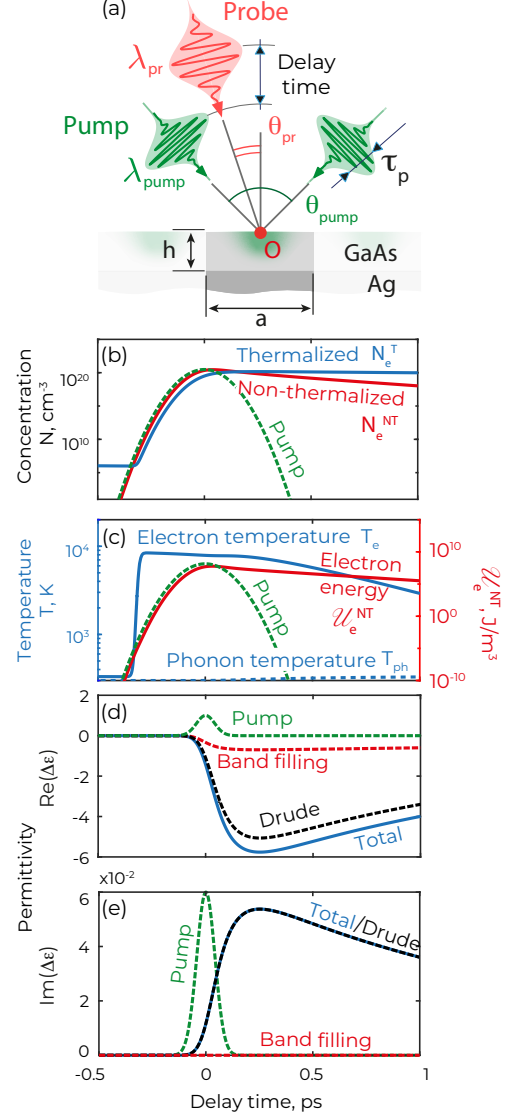


FIG. 2. (a) Interference of two pump beams forming a lattice with period a in GaAs film of height h . The dynamics of non-thermalized N_e^{NT} (b) and thermalized N_e^{T} (c) electrons concentration, energy of non-thermalized electrons U_e^{NT} and electron temperature T_e (d) and phonon temperature T_{ph} computed at the point O in (a). (b) Evolution of real (d) and imaginary (e) parts of the dielectric permittivity correspondent to the wavelength 1600 nm and computed at point O. Drude model (black dashed line) and band filling model (red dashed line) contributions are shown along with their sum ('total', blue solid line). The Gaussian pump profile is shown with a dashed green line.

III. TRANSIENT GRATING FORMATION IN GAAS FILM

We applied developed theoretical model and numerical approach to describe formation of a transient diffraction grating within a GaAs film with a height of $h = 300$ nm on an Ag substrate. To achieve this, we excited the film using two 'pump' plane wave pulses with central wavelength $\lambda_{\text{pump}} = 500$ nm impinging the surface at angles $\theta_{\text{pump}} = \pm 13^\circ$ as shown in Fig. 2 (a). The pulse has Gaussian profile $GP(t) = I_{\text{pump}} \exp(-4 \cdot \ln 2 \cdot t^2 / \tau_p^2)$ reaching the maximal intensity about $I_{\text{pump}} = 10^{14}$ W/m² that leads to significant evolution of the optical parameters of the film, while the pulse duration is set to $\tau_p = 100$ fs. {These pump intensity and pulse duration correspond to a fluence of $F = 1$ mJ/cm², which is below the damage threshold in GaAs [27, 52, 53]. The resulting periodical interference pattern triggers intense generation of non-equilibrium carriers. The period of this interference is $a = 1100$ nm corresponding to the angle of pump incidence of approximately $\theta_{\text{pump}} \approx \arcsin(\lambda_{\text{pump}} / (2a))$.

In Fig. 2, we plot the evolution of non-equilibrium carrier dynamics computed at one point close to the surface (point O in Fig. 2 (a)). At first, the absorbed energy of the pump pulse is transferred to the non-thermalized carriers with rapid growth of their concentration N_e^{NT} (up to the values about 10^{21} cm⁻³, see red solid line in Fig. 2(b)) and energy U_e^{NT} (see red solid line in Fig. 2(c)). After that, at the picosecond timescale, the carriers are being thermalized giving rise to N_e^{T} concentration and carrier temperature T_e (blue solid lines in Fig. 2(b) and (c) correspondingly). The carrier temperature is increased up to the values of $8 \cdot 10^4 - 9 \cdot 10^4$ K and then gradually decreases after the end of the pump pulse due to electron-phonon interactions. At the same time, the phonon temperature increases for less than hundred degrees at this timescale (see blue dashed line in Fig. 2(c)). A more detailed analysis can be found in the Supplemental Information Sec. 4A. Finally, the predicted increase of free carrier concentration results in a drastic change of the complex dielectric permittivity $\text{Re } \varepsilon_{\text{pr}} + i \text{Im } \varepsilon_{\text{pr}}$ at the probe wavelength $\lambda_{\text{pr}} = 1600$ nm as shown in Fig. 2(d) and (e). At the first stage, non-thermalized electrons are generated immediately after the pump pulse arrival. These electrons subsequently undergo thermalization and diffusion, leading to a corresponding modulation of the dielectric constant. One can see that at the current pump intensity, the real part of the permittivity can be reduced for 4-6 units at time scale of 1 ps which constitute almost 50% of the non-perturbed dielectric constant $\varepsilon^0 = 11.4 + i0$ [51]. This variation is predominantly provided by the Drude contribution, while the band filling component is relatively small. The increase in the imaginary part of the permittivity is clearly related to generation of free-carriers, as the impact of the band filling effect is zero for the probe wavelength of 1600 nm, which is higher than the band gap wavelength. At the same time, above the band gap, at the pump wavelength $\lambda_{\text{pump}} = 500$ nm for instance,

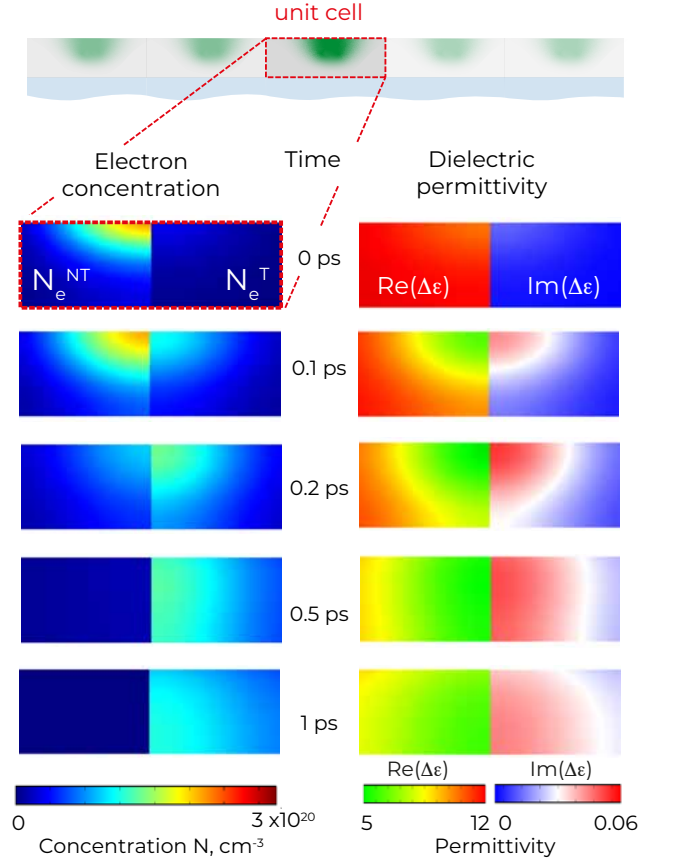


FIG. 3. The distribution of thermalized and non-thermalized electrons concentrations (left column) and real and imaginary parts of dielectric permittivity (right column) for probe wavelength $\lambda_{\text{pr}} = 1600$ nm within the unit cell in GaAs film at different delay time.

both the Drude model and the band filling effect play a substantial role in modulating the dielectric constant of the material (see more details in Supplemental Information Sec. 2C).

While previous simulations show the evolution of dielectric permittivity in time at the given point close to the film interface (point O in Fig. 2 (a)), it is quite insightful to trace the spatial distribution of generated free carriers and correspondent variation of the dielectric permittivity. The left column in Fig. 3 depicts the spatial distribution of the free carriers in a unit cell of the film at different time delays from 0 to 1 ps. One can see that the initially formed non-thermalized electrons are fully converted to thermalized electrons within 0.2 ps at the depth of around $h/2 = 150$ nm, since the thermalization time $\tau_e \approx 200$ fs (See Table I). The thermalized electrons undergo the following diffusion in the depth of the film. The variation of the real and imaginary part of the dielectric permittivity (right column in Fig. 3) generally follows the free-carriers concentration forming an optical grating with high contrast. One can also notice that already at 1 ps delay the optical grating is almost vanished.

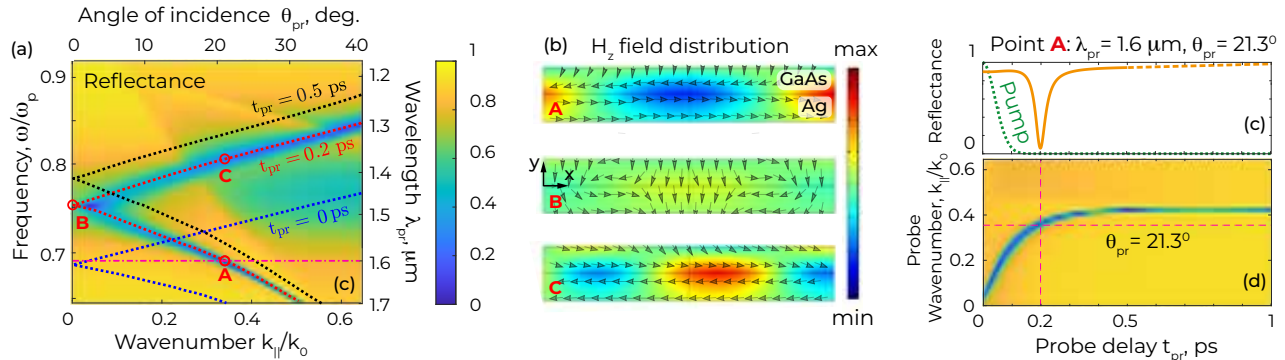


FIG. 4. (a) Reflectance map for the probe irradiation as a function of probe wavelength λ_{pr} and angle of incidence θ_{pr} (frequency $\omega/\omega_p = a/\lambda_{pr}$ and lateral wavenumber $k_{||}/k_0 = \sin(\theta_{pr})$). The map corresponds to a fixed probe time $t_{pr} = 0.2$ ps. The evolution of SPP dispersion over probe time is demonstrated through dashed lines for probe delay time $t_{pr} = 0, 0.2, 0.5$ ps. (b) The magnetic field distribution H_z near the GaAs/Ag interface at a probe delay time $t_{pr} = 0.2$ ps for three specific excitation points labeled as A, B, and C in Fig. 4 (a). The arrows indicate the direction of Poynting vector. (c) The reflectance dynamics for point A ($\lambda_{pr} = 1600$ nm and $\theta_{pr} = 21.3^\circ$). The Gaussian pump profile is shown with a dashed green line. (d) Reflectance map of the probe beam as a function of probe delay time t_{pr} and normalized wavenumber $k_{||}/k_0$ for fixed probe wavelength $\lambda_{pr} = 1600$ nm.

Indeed, the grating contrast if defined by the inhomogeneity of the hot carriers distribution, at the same time within 1 ps the hot carriers become homogeneously distributed across the film driven by diffusion process (See Table I). Note, that the dielectric permittivity of the film is far from the equilibrium ($\text{Re } \epsilon \approx 5$) and it will be kept at this values on the timescale of free carrier recombination, around 5-10 ns. Thus, the lifetime of grating is much faster than the life time of free carriers and is defined by the carrier diffusion time $\tau_{diff}^{N_e}$ (See Table I).

IV. EXCITATION OF SPSS

The optically-induced diffraction grating formed within the GaAs film at picosecond timescale enables the ultrafast excitation of SPPs at the semiconductor/metal interface. As it is widely recognized, SPPs are tightly confined TM electromagnetic surface waves propagating along a metal-semiconductor interface with spectrum lying below the light cone [37]. Therefore, the induced diffraction grating ensures the quasi-phasematching condition and fulfills the quasi-wavevector conservation law, necessary for exciting SPPs from free space [54] as shown in Fig. 1:

$$\frac{2\pi}{a} + k_{pr} \sin(\theta_{pr}) = k_{SPP}(\omega_{pr}). \quad (3)$$

Here, $k_{pr} = \omega_{pr}/c$ is the wavevector of the incident probe, ω_{pr} is the probe frequency, c is the speed of light, $k_{SPP}(\omega_{pr})$ is the dispersion relation of SPP at the probe frequency.

Excitation of SPPs can be observed in the reflectance spectra of the probe beam. For that we plotted the reflectance amplitude as function of the probe wavelength

and incidence angle shown in Fig. 4 (a) at time delay of $t_{pr} = 0.2$ ps after the pump pulse arrival. One can see a distinct dip in the reflectance amplitude corresponding to the excitation of SPP. The SPP dispersion according to Eq.(3) is shown with a red dashed line for the time delay $t_{pr} = 0.2$ ps. This time corresponds to the point of maximum variation in the real part of the dielectric permittivity $\Delta \text{Re } \epsilon_{pr}$, as depicted in Fig. 3.

The distribution of H_z field component for a fixed probe wavelength $\lambda_{pr} = 1600$ nm and angle $\theta_{pr} = 21.3^\circ$ related to the point A in Fig. 4(a) is shown in Fig. 4(b) with a clear signature of SPP mode. The temporal evolution of the reflectance amplitude for the same parameters of the probe wavelength and angle is shown in Fig. 4(c) demonstrating ultrafast excitation of SPP with FWHM about 40 femtoseconds reaching almost zero reflectance. It is worth mentioning that nearly total reduction in reflectance was achieved by adjusting the film thickness of the GaAs film h under fixed pump and probe irradiation conditions ensuring the critical coupling regime. Additionally, at the same angle of incidence $\theta_{pr} = 21.3^\circ$ and probe wavelength $\lambda_{pr} = 1360$ nm (point C) it is feasible to achieve SPP excitation propagating in the opposite direction along the metal-semiconductor interface. The reverse propagation of SPP is indicated by the Poynting vector orientation depicted by arrows in Fig. 4(b) illustrating the energy flow along the interface of the structure. This figure also illustrates the magnetic field distribution H_z at normal incidence of the probing field (point B). The latter relates to the excitation of two oppositely directed SPPs, leading to the formation of a standing SPP wave.

Finally, in Fig. 4(d) we observe that the evolution of the diffraction grating, driven by the diffusion and recombination of induced nonequilibrium carriers in the

conduction band (Fig. 3), causes a shift in the dispersion of the surface plasmon polariton towards shorter wavelength (see in more detail in Supplemental Information Sec. 4C).

This phenomenon opens up an unprecedented way for the ultrafast control over SPPs. Actually, when operating at a fixed wavelength λ_{pr} (for example, 1600 nm) and suitable angle of incidence θ_{pr} (21.3°), the phase matching with SPP is only permitted over the extremely short temporal window at around the intersection between horizontal and vertical dashed lines in Fig. 4(d).

V. CONCLUSION

We theoretically proposed a setup for ultrafast generation of SPP waves at semiconductor film/metal interface by optically induced grating structure. The grating formed in a thin film of GaAs material is induced by the non-equilibrium carriers and exists at the timescales of carriers diffusion that opens an opportunity for ultrafast control over SPP below picosecond time scale. Our re-

sults are based on a developed extended two-temperature self-consistent model that describes the ultrafast optically induced processes in GaAs film and semiconductors in general. In particular, it demonstrates that the optimal delay between the pump pulse generating the grating and the probe pulse exciting the SPP wave, as well as the optimal angle of probe pulse incidence, are fully defined by the carriers dynamics and can be chosen in wide range. Finally, we believe that our advanced theoretical framework concerning ultrafast semiconductor responses to pulsed electromagnetic radiation and proposed novel technique for ultrafast SSP control exhibit significant potential for diverse applications in all-optically controlled ultrafast devices.

VI. ACKNOWLEDGEMENT

The authors are thankful Yonatan Sivan and Zarina Sadrieva for fruitful discussions. The work was supported by the Federal Academic Leadership Program Priority 2030.

-
- [1] A. I. Kuznetsov, A. E. Miroschnichenko, M. L. Brongersma, Y. S. Kivshar, and B. Luk'yanchuk, "Optically resonant dielectric nanostructures," *Science*, vol. 354, no. 6314, p. aag2472, 2016.
- [2] Y. Kivshar, "All-dielectric meta-optics and non-linear nanophotonics," *National Science Review*, vol. 5, no. 2, pp. 144–158, 2018.
- [3] K. Koshelev, S. Kruk, E. Melik-Gaykazyan, J.-H. Choi, A. Bogdanov, H.-G. Park, and Y. Kivshar, "Subwavelength dielectric resonators for nonlinear nanophotonics," *Science*, vol. 367, no. 6475, pp. 288–292, 2020.
- [4] D. Smirnova and Y. S. Kivshar, "Multipolar nonlinear nanophotonics," *Optica*, vol. 3, no. 11, pp. 1241–1255, 2016.
- [5] G. Grinblat, "Nonlinear dielectric nanoantennas and metasurfaces: frequency conversion and wavefront control," *ACS Photonics*, vol. 8, no. 12, pp. 3406–3432, 2021.
- [6] E. A. A. Pogna, M. Celebrano, A. Mazzanti, L. Ghirardini, L. Carletti, G. Marino, A. Schirato, D. Viola, P. Laporta, C. De Angelis, *et al.*, "Ultrafast, all optically reconfigurable, nonlinear nanoantenna," *ACS nano*, vol. 15, no. 7, pp. 11150–11157, 2021.
- [7] S. Makarov, S. Kudryashov, I. Mukhin, A. Mozharov, V. Milichko, A. Krasnok, and P. Belov, "Tuning of magnetic optical response in a dielectric nanoparticle by ultrafast photoexcitation of dense electron-hole plasma," *Nano letters*, vol. 15, no. 9, pp. 6187–6192, 2015.
- [8] M. Maiuri, A. Schirato, G. Cerullo, and G. Della Valle, "Ultrafast all-optical metasurfaces: challenges and new frontiers," *ACS Photonics*, vol. 11, no. 8, pp. 2888–2905, 2024.
- [9] M. R. Shcherbakov, S. Liu, V. V. Zubyuk, A. Vaskin, P. P. Vabishchevich, G. Keeler, T. Pertsch, T. V. Dolgova, I. Staude, I. Brener, *et al.*, "Ultrafast all-optical tuning of direct-gap semiconductor metasurfaces," *Nature communications*, vol. 8, no. 1, pp. 1–6, 2017.
- [10] I. S. Sinev, K. Koshelev, Z. Liu, A. Rudenko, K. Ladutenko, A. Shcherbakov, Z. Sadrieva, M. Baranov, T. Itina, J. Liu, *et al.*, "Observation of ultrafast self-action effects in quasi-bic resonant metasurfaces," *Nano Letters*, vol. 21, no. 20, pp. 8848–8855, 2021.
- [11] M. R. Shcherbakov, P. P. Vabishchevich, A. S. Shorokhov, K. E. Chong, D.-Y. Choi, I. Staude, A. E. Miroschnichenko, D. N. Neshev, A. A. Fedyanin, and Y. S. Kivshar, "Ultrafast all-optical switching with magnetic resonances in nonlinear dielectric nanostructures," *Nano letters*, vol. 15, no. 10, pp. 6985–6990, 2015.
- [12] Z. Zheng, D. Rocco, H. Ren, O. Sergaeva, Y. Zhang, K. B. Whaley, C. Ying, D. de Ceglia, C. De-Angelis, M. Rahmani, *et al.*, "Advances in nonlinear metasurfaces for imaging, quantum, and sensing applications," *Nanophotonics*, vol. 12, no. 23, pp. 4255–4281, 2023.
- [13] S. Gennaro, R. Sarma, and I. Brener, "Nonlinear and ultrafast all-dielectric metasurfaces at the center for integrated nanotechnologies," *Nanotechnology*, vol. 33, no. 40, p. 402001, 2022.
- [14] Z. Yang, M. Liu, D. Smirnova, A. Komar, M. Shcherbakov, T. Pertsch, and D. Neshev, "Ultrafast q-boosting in semiconductor metasurfaces," *Nanophotonics*, vol. 13, no. 12, pp. 2173–2182, 2024.
- [15] G. Della Valle, B. Hopkins, L. Ganzer, T. Stoll, M. Rahmani, S. Longhi, Y. S. Kivshar, C. De Angelis, D. N. Neshev, and G. Cerullo, "Nonlinear anisotropic dielectric metasurfaces for ultrafast nanophotonics," *ACS Photonics*, vol. 4, no. 9, pp. 2129–2136, 2017.
- [16] D. A. Shilkin, S. T. Ha, R. Paniagua-Domínguez, and A. I. Kuznetsov, "Ultrafast modulation of a nonlocal semiconductor metasurface under spatially selective optical pumping," *Nano Letters*, 2024.

- [17] M. Celebrano, D. Rocco, M. Gandolfi, A. Zilli, F. Rusconi, A. Tognazzi, A. Mazzanti, L. Ghirardini, E. A. Pogna, L. Carletti, *et al.*, “Optical tuning of dielectric nanoantennas for thermo-optically reconfigurable nonlinear metasurfaces,” *Optics Letters*, vol. 46, no. 10, pp. 2453–2456, 2021.
- [18] D. Rocco, M. Gandolfi, A. Tognazzi, O. Pashina, G. Zograf, K. Frizyuk, C. Gigli, G. Leo, S. Makarov, M. Petrov, *et al.*, “Opto-thermally controlled beam steering in nonlinear all-dielectric metastructures,” *Optics Express*, vol. 29, no. 23, pp. 37128–37139, 2021.
- [19] T. V. Tsoulos and G. Tagliabue, “Self-induced thermo-optical effects in silicon and germanium dielectric nanoresonators,” *Nanophotonics*, vol. 9, no. 12, pp. 3849–3861, 2020.
- [20] M. Rahmani, L. Xu, A. E. Miroshnichenko, A. Komar, R. Camacho-Morales, H. Chen, Y. Zárate, S. Kruk, G. Zhang, D. N. Neshev, *et al.*, “Reversible thermal tuning of all-dielectric metasurfaces,” *Advanced Functional Materials*, vol. 27, no. 31, p. 1700580, 2017.
- [21] T. Zhang, Y. Che, K. Chen, J. Xu, Y. Xu, T. Wen, G. Lu, X. Liu, B. Wang, X. Xu, *et al.*, “Anapole mediated giant photothermal nonlinearity in nanostructured silicon,” *Nature communications*, vol. 11, no. 1, p. 3027, 2020.
- [22] Y.-S. Duh, Y. Nagasaki, Y.-L. Tang, P.-H. Wu, H.-Y. Cheng, T.-H. Yen, H.-X. Ding, K. Nishida, I. Hotta, J.-H. Yang, *et al.*, “Giant photothermal nonlinearity in a single silicon nanostructure,” *Nature communications*, vol. 11, no. 1, p. 4101, 2020.
- [23] K. Nishida, P.-H. Tseng, Y.-C. Chen, P.-H. Wu, C.-Y. Yang, J.-H. Yang, W.-R. Chen, O. Pashina, M. I. Petrov, K.-P. Chen, *et al.*, “Optical bistability in nanosilicon with record low q -factor,” *Nano Letters*, vol. 23, no. 24, pp. 11727–11733, 2023.
- [24] G. P. Zograf, M. I. Petrov, S. V. Makarov, and Y. S. Kivshar, “All-dielectric thermonanophotonics,” *Advances in Optics and Photonics*, vol. 13, no. 3, pp. 643–702, 2021.
- [25] D. Ryabov, O. Pashina, G. Zograf, S. Makarov, and M. Petrov, “Nonlinear optical heating of all-dielectric super-cavity: efficient light-to-heat conversion through giant thermorefractive bistability,” *Nanophotonics*, vol. 11, no. 17, pp. 3981–3991, 2022.
- [26] C. Husko and C. W. Wong, “Ultrafast all-optical bistability in algaas photonic crystals,” in *Nanophotonics for Communication: Materials, Devices, and Systems III*, vol. 6393, pp. 111–117, SPIE, 2006.
- [27] A. Di Cicco, G. Polzoni, R. Gunnella, A. Trapananti, M. Minicucci, S. Rezvani, D. Catone, L. Di Mario, J. Pelli Cresi, S. Turchini, *et al.*, “Broadband optical ultrafast reflectivity of si, ge and gaas,” *Scientific Reports*, vol. 10, no. 1, p. 17363, 2020.
- [28] G. Crotti, M. Akturk, A. Schirato, V. Vinel, A. A. Trifonov, I. C. Buchvarov, D. N. Neshev, R. Proietti Zaccaria, P. Laporta, A. Lemaitre, *et al.*, “Giant ultrafast dichroism and birefringence with active nonlocal metasurfaces,” *Light: Science & Applications*, vol. 13, no. 1, p. 204, 2024.
- [29] A. Tognazzi, P. Franceschini, O. Sergaeva, L. Carletti, I. Alessandri, G. Finco, O. Takayama, R. Malureanu, A. V. Lavrinenko, A. C. Cino, *et al.*, “Giant photoinduced reflectivity modulation of nonlocal resonances in silicon metasurfaces,” *Advanced Photonics*, vol. 5, no. 6, pp. 066006–066006, 2023.
- [30] Y. Yang, W. Wang, A. Boulesbaa, I. I. Kravchenko, D. P. Briggs, A. Poretzky, D. Geohegan, and J. Valentine, “Nonlinear fano-resonant dielectric metasurfaces,” *Nano letters*, vol. 15, no. 11, pp. 7388–7393, 2015.
- [31] M. A. Masharin, T. Oskolkova, F. Isik, H. Volkan Demir, A. K. Samusev, and S. V. Makarov, “Giant ultrafast all-optical modulation based on exceptional points in exciton–polariton perovskite metasurfaces,” *ACS nano*, vol. 18, no. 4, pp. 3447–3455, 2024.
- [32] R. Berté, T. Possmayer, A. Tittl, L. d. S. Menezes, and S. A. Maier, “Emergent resonances in a thin film tailored by optically-induced small permittivity asymmetries,” *arXiv preprint arXiv:2403.05730*, 2024.
- [33] I. Staude, T. Pertsch, and Y. S. Kivshar, “All-dielectric resonant meta-optics lightens up,” *Acs Photonics*, vol. 6, no. 4, pp. 802–814, 2019.
- [34] Y. Sivan and M. Spector, “Ultrafast dynamics of optically induced heat gratings in metals,” *ACS Photonics*, vol. 7, no. 5, pp. 1271–1279, 2020.
- [35] A. Schirato, M. Maiuri, A. Toma, S. Fugattini, R. Proietti Zaccaria, P. Laporta, P. Nordlander, G. Cerullo, A. Alabastri, and G. Della Valle, “Transient optical symmetry breaking for ultrafast broadband dichroism in plasmonic metasurfaces,” *Nature Photonics*, vol. 14, p. 723–727, Oct. 2020.
- [36] A. Schirato, G. Crotti, R. Proietti Zaccaria, A. Alabastri, and G. Della Valle, “Hot carrier spatio-temporal inhomogeneities in ultrafast nanophotonics,” *New Journal of Physics*, vol. 24, p. 045001, Apr. 2022.
- [37] L. Zheng, U. Zywiets, A. Evlyukhin, B. Roth, L. Overmeyer, and C. Reinhardt, “Experimental Demonstration of Surface Plasmon Polaritons Reflection and Transmission Effects,” *Sensors*, vol. 19, p. 4633, Oct. 2019.
- [38] Y. Dubi and Y. Sivan, ““hot” electrons in metallic nanostructures—non-thermal carriers or heating?,” *Light: Science & Applications*, vol. 8, no. 1, p. 89, 2019.
- [39] K. Oguri, T. Tsunoi, K. Kato, H. Nakano, T. Nishikawa, K. Tateno, T. Sogawa, and H. Gotoh, “Dynamical observation of photo-dember effect on semi-insulating gaas using femtosecond core-level photoelectron spectroscopy,” *Applied Physics Express*, vol. 8, no. 2, p. 022401, 2015.
- [40] B. Schumann, “Properties of Gallium Arsenide. EMIS Datareviews Series no. 2, second edition. INSPEC, The Institute of Electric Engineering, London and New York 1990, 790 + XXIV Seiten, zahlreiche Tabellen und Literaturangaben, Sachwortverzeichnis, ISBN 0-85296-485-4,” *Cryst. Res. Technol.*, vol. 26, p. 18, Jan. 1991.
- [41] T. J.-Y. Derrien, T. Sarnet, M. Sentis, and T. E. Itina, “Application of a two-temperature model for the investigation of the periodic structure formation on Si surface in femtosecond laser interaction,” *J. Optoelectron. Adv. Mater.*, vol. 12, pp. 610–615, oct 2011.
- [42] ioffe.ru GaAs, “Physical properties of Gallium Arsenide (GaAs),” July 2001. [Online; accessed 18. Nov. 2022].
- [43] R. A. Höpfel, J. Shah, P. A. Wolff, and A. C. Gossard, “Electron-hole scattering in GaAs quantum wells,” *Phys. Rev. B*, vol. 37, pp. 6941–6954, apr 1988.
- [44] Y. Sivan and M. Spector, “Ultrafast Dynamics of Optically Induced Heat Gratings in Metals,” *ACS Photonics*, vol. 7, pp. 1271–1279, May 2020.
- [45] A. Margiolakis, G. D. Tsibidis, K. M. Dani, and G. P. Tsironis, “Ultrafast dynamics and subwavelength periodic structure formation following irradiation of GaAs with femtosecond laser pulses,” *Phys. Rev. B*, vol. 98,

- p. 224103, Dec. 2018.
- [46] B. A. Ruzicka, L. K. Werake, H. Samassekou, and H. Zhao, "Ambipolar diffusion of photoexcited carriers in bulk GaAs," *Appl. Phys. Lett.*, vol. 97, Dec. 2010.
- [47] U. Strauss, W. W. Rühle, and K. Köhler, "Auger recombination in intrinsic GaAs," *Appl. Phys. Lett.*, vol. 62, pp. 55–57, Jan. 1993.
- [48] A. Block, M. Liebel, R. Yu, M. Spector, Y. Sivan, F. García de Abajo, and N. F. van Hulst, "Tracking ultrafast hot-electron diffusion in space and time by ultrafast thermomodulation microscopy," *Science advances*, vol. 5, no. 5, p. eaav8965, 2019.
- [49] K. Sokolowski-Tinten and D. von der Linde, "Generation of dense electron-hole plasmas in silicon," *Phys. Rev. B*, vol. 61, pp. 2643–2650, Jan. 2000.
- [50] B. Bennett, R. Soref, and J. Alamo, "Carrier-induced change in refractive index of InP, GaAs and InGaAsP," *Quantum Electronics, IEEE Journal of*, vol. 26, pp. 113–122, Feb. 1990.
- [51] K. Papatryfonos, T. Angelova, A. Brimont, B. Reid, S. Guldin, P. Smith, M. Tang, K. Li, A. Seeds, H. Liu, and D. Selviah, "Refractive indices of MBE-grown Al x Ga (1- x) As ternary alloys in the transparent wavelength region," *AIP Adv.*, vol. 11, p. 025327, Feb. 2021.
- [52] E. Glezer, Y. Siegal, L. Huang, and E. Mazur, "Laser-induced band-gap collapse in gaas," *Physical Review B*, vol. 51, no. 11, p. 6959, 1995.
- [53] A. P. Singh, A. Kapoor, and K. Tripathi, "Ripples and grain formation in gaas surfaces exposed to ultrashort laser pulses," *Optics & Laser Technology*, vol. 34, no. 7, pp. 533–540, 2002.
- [54] G. Liang, Z. Luo, K. Liu, Y. Wang, D. Jianxiong, and Y. Duan, "Fiber Optic Surface Plasmon Resonance-Based Biosensor Technique: Fabrication, Advancement, and Application," *Crit. Rev. Anal. Chem.*, vol. 46, p. 00, Nov. 2015.